Cell Stem Cell
Article

The Histone Acetyltransferase MOF Is a Key Regulator of the Embryonic Stem Cell Core Transcriptional Network

Xiangzhi Li,[1,2,6] Li Li,[4,6] Ruchi Pandey,[2] Jung S. Byun,[5] Kevin Gardner,[5] Zhaohui Qin,[4] and Yali Dou[2,3,*]
[1]Institute of Cell Biology, School of Medicine, Shandong University, Shandong 250100, China
[2]Department of Pathology
[3]Department of Biological Chemistry
University of Michigan, Ann Arbor, MI 48109, USA
[4]Department of Biostatistics and Bioinformatics, Rollins School of Public Health, Emory University, Atlanta, GA 30322, USA
[5]Laboratory of Gene Expression, NIH, Bethesda, MD 20892, USA
[6]These authors contributed equally to this work
*Correspondence: yalid@umich.edu
http://dx.doi.org/10.1016/j.stem.2012.04.023

SUMMARY

Pluripotent embryonic stem cells (ESCs) maintain self-renewal and the potential for rapid response to differentiation cues. Both ESC features are subject to epigenetic regulation. Here we show that the histone acetyltransferase Mof plays an essential role in the maintenance of ESC self-renewal and pluripotency. ESCs with Mof deletion lose characteristic morphology, alkaline phosphatase (AP) staining, and differentiation potential. They also have aberrant expression of the core transcription factors Nanog, Oct4, and Sox2. Importantly, the phenotypes of Mof null ESCs can be partially suppressed by Nanog overexpression, supporting the idea that Mof functions as an upstream regulator of Nanog in ESCs. Genome-wide ChIP-sequencing and transcriptome analyses further demonstrate that Mof is an integral component of the ESC core transcriptional network and that Mof primes genes for diverse developmental programs. Mof is also required for Wdr5 recruitment and H3K4 methylation at key regulatory loci, highlighting the complexity and interconnectivity of various chromatin regulators in ESCs.

INTRODUCTION

Embryonic stem cells (ESCs) are pluripotent cells capable of indefinite self-renewal and differentiation into all cell types. The maintenance of ESC pluripotency status requires specific core transcription factors, such as Oct4 (also known as Pou5f1), Sox2, and Nanog, which are the cornerstones of an intricate and highly interconnected ESC transcriptional network or core regulatory circuitry (Chen et al., 2008; Macarthur et al., 2009; Orkin et al., 2008). They recruit multiple chromatin regulatory factors or complexes to promote activation of stemness genes while simultaneously allowing for repression of differentiation genes (Orkin and Hochedlinger, 2011; Young, 2011). Two antagonistic chromatin methylation activities (i.e., Polycomb repression complex 2 [PRC2] and MLL family complexes) are shown to function coordinately with these core transcription factors in ESCs. The PRC2 complex methylates histone H3K27 and functions to silence developmentally regulated genes. On the other hand, MLL family histone methyltransferases (HMTs) deposit histone H3K4 methylation, which keeps lineage-specific genes poised for activation as cells enter various differentiation pathways. The significance of H3K4 and H3K27 methylation in regulating the ESC transcription program is best exemplified by the presence of "bivalent domains" at many important regulatory regions, defined by high levels of both H3K4 and H3K27 trimethylation. These bivalent domains are evolutionarily conserved and their resolution during ESC differentiation serves to commit ESCs into a specific lineage (Azuara et al., 2006; Bernstein et al., 2006; Pan et al., 2007).

In addition to histone methylation, the pluripotency status of ESCs is also regulated by histone acetylation. Addition of histone deacetylase (HDAC) inhibitors prevents ESC differentiation and increases the efficiency of induced pluripotent stem cell (iPSC) induction (Feng et al., 2009). Histone acetylation also supports "hyper-dynamic" chromatin conformation (Meshorer, 2007; Niwa, 2007) and hyperactive transcription states (Efroni et al., 2008), two common signatures of pluripotent cells. Upon differentiation, the chromatin structure of ESCs becomes more compact and overall transcription is reduced (Aoto et al., 2006; Park et al., 2004). This process is accompanied by global reduction of panacetylation of histones H3 and H4 (Kobayakawa et al., 2007). Consistent with the importance of histone acetylation in ESC function, genetic ablation or knockdown of several histone acetyltransferases (HATs) such as Tip60, p300, and Gcn5 led to aberrant expression of lineage-specific genes and profound defects in ESC differentiation (Chen et al., 2008; Fazzio et al., 2008; Lin et al., 2007; Zhong and Jin, 2009). Notably, these HATs do not affect expression of the core pluripotency factors Oct4, Nanog, and Sox2 (Fazzio et al., 2008; Lin et al., 2007; Zhong and Jin, 2009). Instead, they function mostly at downstream differentiation processes.

HAT Mof (also called MYST1 or KAT8) is a highly conserved MYST family HAT. MOF was originally described as an essential component of the X chromosome dosage compensation

complex (DCC) in *Drosophila,* causing a 2-fold increase in expression of X-linked genes in male flies (Conrad and Akhtar, 2011; Gelbart and Kuroda, 2009; Lucchesi et al., 2005). In mammals, MOF is essential for vertebrate development and constitutive ablation of *Mof* leads to peri-implantation lethality in mouse embryos (Gupta et al., 2008; Thomas et al., 2008). $Mof^{-/-}$ embryos showed massive abnormal chromatin aggregations, suggesting a crucial role for *Mof* in maintenance of chromatin structures in vivo. Mammalian MOF was initially purified in a WDR5-containing complex (Dou et al., 2005). Later in vitro biochemical studies show that MOF resides in two distinct complexes in mammals: the MOF-MSL complex and the MOF-MSL1v1 complex (Li and Dou, 2010), which are either physically or functionally connected with H3K4 methyltransferase MLL. In brief, the MOF-MSL1v1 complex physically interacts with the MLL complex through the commonly shared component WDR5 and coordinates with MLL in transcription activation (Dou et al., 2005; Li et al., 2009); On the other hand, the MOF-MSL complex is able to stimulate H3K4me3 through H2BK34ub-mediated *trans*-tail regulation (Wu et al., 2011). Given the close connection of MOF and H3K4 methylation, the direct interaction between MOF and WDR5, and the recent demonstration that WDR5 mediates self-renewal and reprogramming (Ang et al., 2011), we decided to examine whether MOF plays a role in ESC fate determination and whether MOF-mediated H4 acetylation contributes to ESC pluripotency.

Using the conditional knockout ESC lines for Mof, here we show that Mof is essential for ESC self-renewal and pluripotency. Mof deletion leads to loss of ESC self-renewal and defects in embryoid body (EB) formation, which are accompanied by reduced H4K16 acetylation (K16ac) and global changes in ESC transcriptome. Importantly, unlike other HATs, Mof directly regulates expression of the core ESC transcription factors Nanog, Oct4, and Sox2, and Mof null phenotypes can be partially rescued by ectopic Nanog expression. All together, our data provide strong support for a critical and unique role of Mof in regulating the ESC core transcriptional network.

RESULTS

Mof Expression and H4K16ac Are Downregulated during ESC Differentiation

Recent studies show that histone modifications, especially histone H3K4me3 and H3K27me3, play important roles in regulating ESC self-renewal and pluoripotency. Given the interaction of MOF with MLL (Dou et al., 2005) and the correlation of H3K4me3 and H4K16ac at transcriptionally active genes (Ruthenburg et al., 2011), we decided to examine whether Mof and its acetyltransferase activity play a role in murine ESC functions. To this end, we first compared levels of Mof and H4K16ac in ESCs to those of mouse embryonic fibroblasts (MEFs). As shown in Figure 1A, the levels of Mof and H4K16ac were significantly higher in ESCs than those in MEFs. Differences in histone H3K4me3 and H3K27me3 in ESCs versus MEFs were moderate in comparison (Figure 1A). Furthermore, when ESCs were subjected to either retinoic acid (RA)-induced differentiation (Figures 1B and 1C) or spontaneous differentiation (Figures 1D and 1E), Mof transcript and protein levels were gradually downregulated, which were in parallel with downregulation of ESC pluripotency genes Pou5f1 (Oct4) and Nanog (Figures 1B and 1D). As a control, we also observed a similar downregulation of Wdr5 in differentiating ESCs, consistent with the previous report (Ang et al., 2011).

Establishing 4-OHT-Inducible Mof Knockout ESC Lines

Downregulation of *Mof* expression during ESC differentiation is intriguing because this process is concomitant with changes in chromatin conformation and dynamism (Gaspar-Maia et al., 2011). To determine the role of Mof in ESCs, we derived inducible Mof knockout ESC lines from the $Mof^{flox/flox}$, $Cre\text{-}ER^{TM}$ mouse model we previously described (Li et al., 2010). In this model, floxed *Mof* alleles (i.e., exons 4–6) can be deleted upon 4-OHT-induced expression of Cre recombinase (Figure 2A). This leads to Mof protein degradation and loss of global H4K16ac (Li et al., 2010). The primary ESC lines including $Cre\text{-}ER^{TM}$-positive $Mof^{flox/flox}$, $Mof^{flox/+}$, and $Mof^{+/+}$ were obtained from E3.5 dpc embryos after intercrossing $Mof^{flox/+}$, $Cre\text{-}ER^{TM}$ mice (Figure 2A). Successful generation of $Mof^{+/+}$, $Mof^{+/-}$, and $Mof^{-/-}$ ESCs was confirmed by genotyping and immunoblots (Figures 2A and 2B). For Mof deletion, these cells were subjected to continuous 4-OHT treatments for 4 days. As shown in Figure S1A (available online), day 4 is the earliest time point at which we were able to achieve complete Mof deletion and observe significant reduction in the Mof protein level. We decided to use this time point for all the experiments described in this study. Consistent with the role of Mof and H4K16ac in regulating higher-order chromatin structures (Robinson et al., 2008; Shogren-Knaak et al., 2006), Mof deletion led to massive chromatin compaction with significant increase of densely stained heterochromatin in the nucleus as observed by electron microscopy studies (Figure 2C). Mof deletion eventually led to growth arrest and cell death of ESCs (Figure S1B). However, the chromatin aggregation shown here (day 4) was not a result of cell death. At this time point, the cell cycle index of *Mof* knockout ESCs was comparable to that of wild-type cells (Figures S1C–S1E). The generation of inducible *Mof* knockout ESC lines allowed us to study the effects of *Mof* deletion on ESC functions in a defined genetic background.

Mof Is Required for ESC Self-Renewal and Differentiation

Apparent changes in ESC morphology were observed upon Mof deletion. $Mof^{-/-}$ ESCs became flattened and elongated with reduced cell-cell contacts and failed to form compact colonies in culture (Figure 2D, right panel). These morphological changes were not due to defects in ESC proliferation because similar changes, albeit to a less extent, were also observed for $Mof^{+/-}$ ESCs (Figure 2D, middle panel), which had no detectable growth differences from the wild-type cells (Figure S1F and data not shown).

Consistent with morphological changes, $Mof^{-/-}$ ESCs had very weak AP staining compared to that of $Mof^{+/+}$ and $Mof^{+/-}$ ESCs (Figure 2D), suggesting loss of ESC self-renewal capability. A moderate decrease of AP staining was also observed for $Mof^{+/-}$ cells (Figure 2D and Figure S2A). We further examined the ability of $Mof^{-/-}$ ESCs to aggregate in suspension to form EBs. As shown in Figure 2E, $Mof^{-/-}$ ESCs failed to aggregate and most cells remained dispersed in suspension culture. In

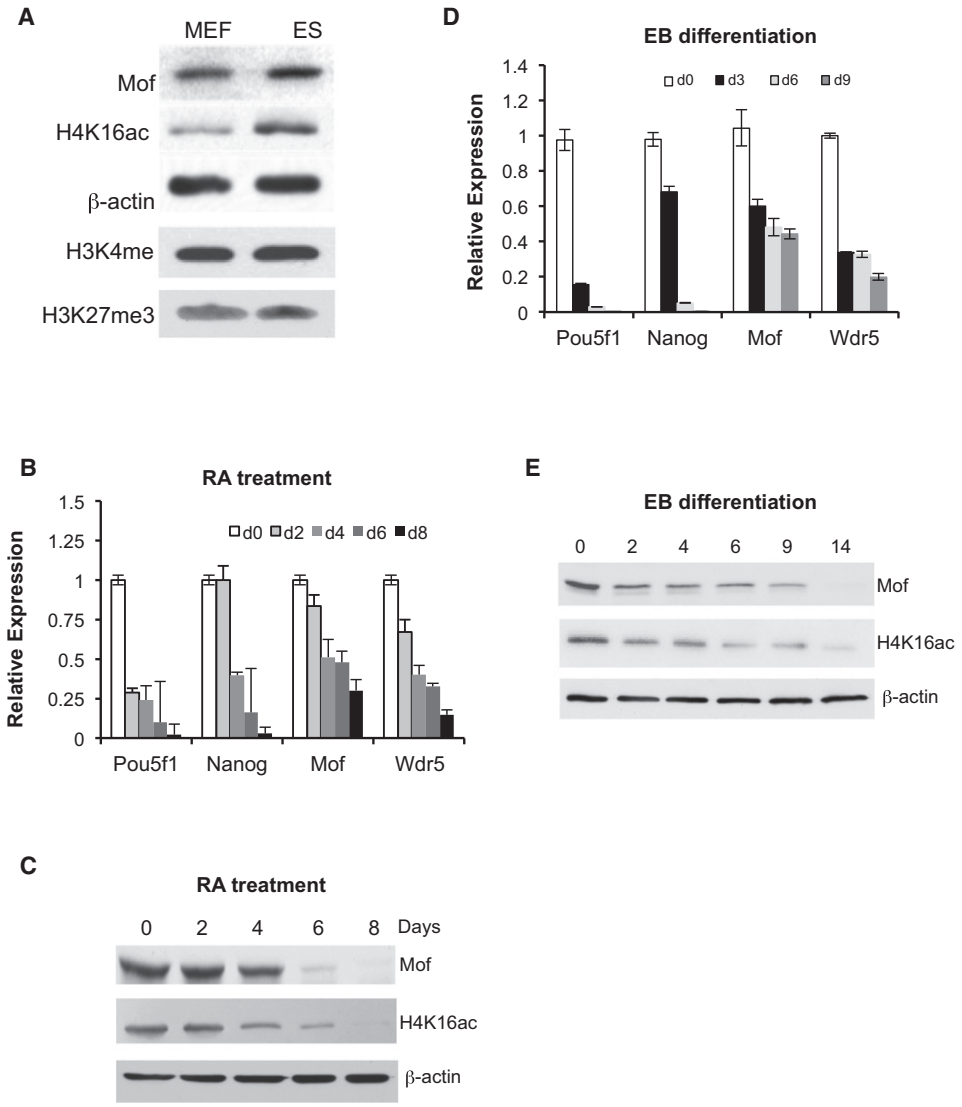

Figure 1. Mof Is Downregulated during ESC Differentiation

(A) Immunoblots for proteins from mouse embryonic fibroblasts (MEFs) and embryonic stem cells (ESCs) as indicated on top. Antibodies are indicated at left. (B) Real-time PCR and (C) immunoblot analyses for RA-induced ESC differentiation. (D) Real-time PCR and (E) immunoblot analyses for ESC differentiation during EB formation. In (B) and (D), fold changes of each transcript relative to its expression in day 0 EB formation are presented. For (C) and (E), β-actin was used as the loading control.

contrast, both *Mof*$^{+/+}$ and *Mof*$^{+/-}$ ESCs efficiently aggregated and eventually developed into cystic structures (Figure 2E and data not shown). We further examined differentiation of three primitive germ layers in *Mof*$^{+/-}$ EBs. We found that expression of marker genes for all three germ layers was downregulated in *Mof*$^{+/-}$ EBs (Figures S2B–S2E). The effects of deleting one Mof allele were moderate, consistent with largely normal phenotypes of *Mof*$^{+/-}$ mice (data not shown). Because *Mof* $^{-/-}$ ESCs were not able to form EBs, we decided to delete Mof after ESC aggregation and examine whether Mof played a role at later differentiation steps. We examined expression of hematopoietic genes (i.e., Tal1, Lmo2, and Runx1), which were highly expressed in late EBs. These genes were significantly compromised in *Mof* $^{-/-}$ EBs, suggesting impairment of hematopoietic differentiation (Figure S3A). Taken together, ESCs with Mof deletion had defects in several characteristic features of stem cells: morphology, AP activity, and EB formation/differentiation. These results suggest that Mof is essential for ESC functions.

Mof Deletion Led to Aberrant Expression of ESC Core Transcription Factors and Differentiation Marker Genes

To gain insights into the function of Mof in ESCs and to rule out the possibility that loss of self-renewal and pluripotency observed in *Mof*$^{-/-}$ cells was due to a general defect in cell proliferation and/or increased apoptosis, we performed gene expression analyses for *Mof*$^{+/+}$ and *Mof*$^{-/-}$ ESCs by microarray. We found that Mof deletion had profound impacts on the ESC

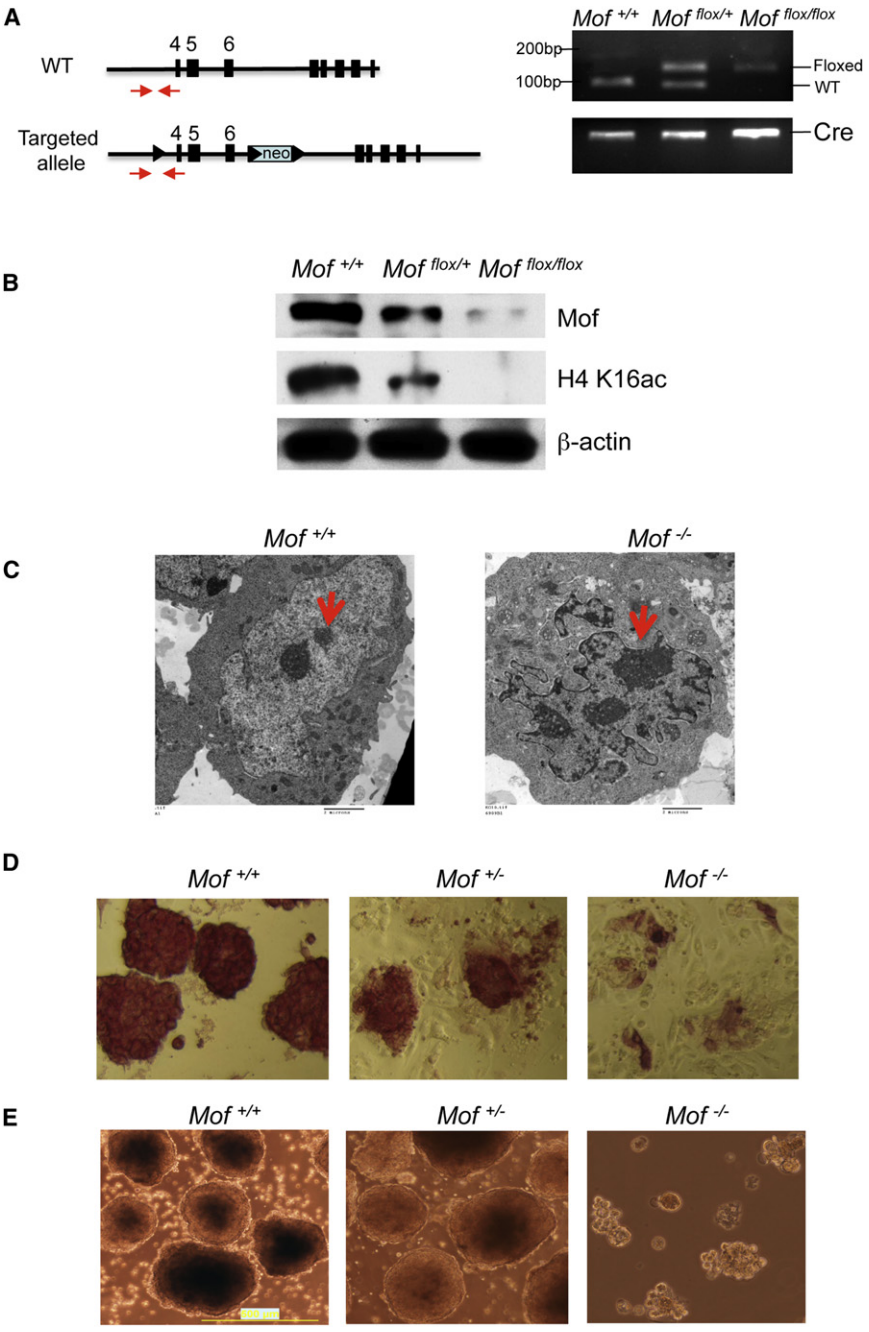

Figure 2. Mof Is Essential for ESC Self-Renewal

(A) Left, schematic for wild-type and Mof knockout alleles. Genotyping primers (red arrows) are indicated. Right, genotyping results for wild-type, floxed Mof alleles as well as *Cre-ER*^{TM} by PCR.

(B) Immunoblots for Mof and H4K16ac in *Mof*$^{+/+}$, *Mof*$^{flox/+}$, and *Mof*$^{flox/flox}$ cells after 4-OHT treatment. Immunoblot for β-actin was used as the loading control.

(C) Electron microscopy images of wild-type (left) and Mof knockout nuclei (right). Densely stained heterochromatin is indicated by arrow. Scale bars, 2 μm.

(D) Alkaline phosphatase staining of *Mof*$^{+/+}$, *Mof*$^{+/-}$, and *Mof*$^{-/-}$ ESCs.

(E) Light microscopy images of day 4 EB for *Mof*$^{+/+}$, *Mof*$^{+/-}$, and *Mof*$^{-/-}$ ESCs. Scale bars, 0.5 mm. Also see Figure S1.

transcriptome. There were 4,475 genes that were differentially expressed by more than 2-fold upon Mof deletion (Table S1 and Table S2). About an equal number of genes were up- (2,081) or down- (2,394) regulated in *Mof*$^{-/-}$ ESCs (Table S1 and Table S2). Of note, fold changes in gene expression upon Mof deletion were generally small, with mean fold change at ~2.8 (Figure 7C, total) for both upregulated and downregulated genes. Consistent with Mof playing an important role in ESCs, we found changes in expression of Oct4, Nanog, and most of their conserved joint targets (Figure 3A and Loh et al., 2006). Most of these genes (e.g., Oct4, Nanog, Rif1, Esrrb, Zic3, Tcf7, Jarid2, and Rest) were significantly downregulated with the exception of Klf4 and Myc, whose expressions were increased. Microarray results for key ESC regulators were confirmed by RT-PCR (Figure 3B). In addition to changes in expression of ESC core transcription factors, Mof deletion also led to aberrant expression of differentiation markers for all three primitive germ layers. They included Sox17, Foxa2, Gata6, and Gata4 for primitive endoderm, T/Bra and Lhx1 for primitive mesoderm, and Sox1, Pax3, Otx2, and Nestin for neuroectoderm (Figure 3C). Most of these differentiation genes were upregulated, supporting the idea that Mof null phenotypes were not simply due to general loss of cell viability.

To examine whether genes with changed expression were direct Mof targets, we performed ChIP analyses for Mof and H4K16ac on selected gene promoters. As shown in Figure 3D, Mof directly bound to pluripotency genes including Nanog, Pou5f1, Sox2, Fgf4, Lefty1, and Tcl1 (Figure 3D). Downregulation of these genes in *Mof*$^{-/-}$ ESCs (Figure 3B) coincided with loss of Mof binding and H4K16ac (Figure 3D). Our result that Mof directly regulates Nanog and Oct4 makes Mof a unique HAT in regulating ESC self-renewal genes. In contrast, all other HATs studied insofar, including Tip60, Gcn5, and p300/CBP, showed little effects on transcription of Oct4, Nanog, and Sox2 after knockout or knockdown. Instead, they were important for regulating downstream ESC differentiation processes (Fazzio et al., 2008; Lin et al., 2007; Zhong and Jin, 2009). In addition to examining Mof binding at ESC core transcription factor loci, we also checked Mof binding at several genes whose expression was upregulated by Mof deletion. Surprisingly, we found that some of the

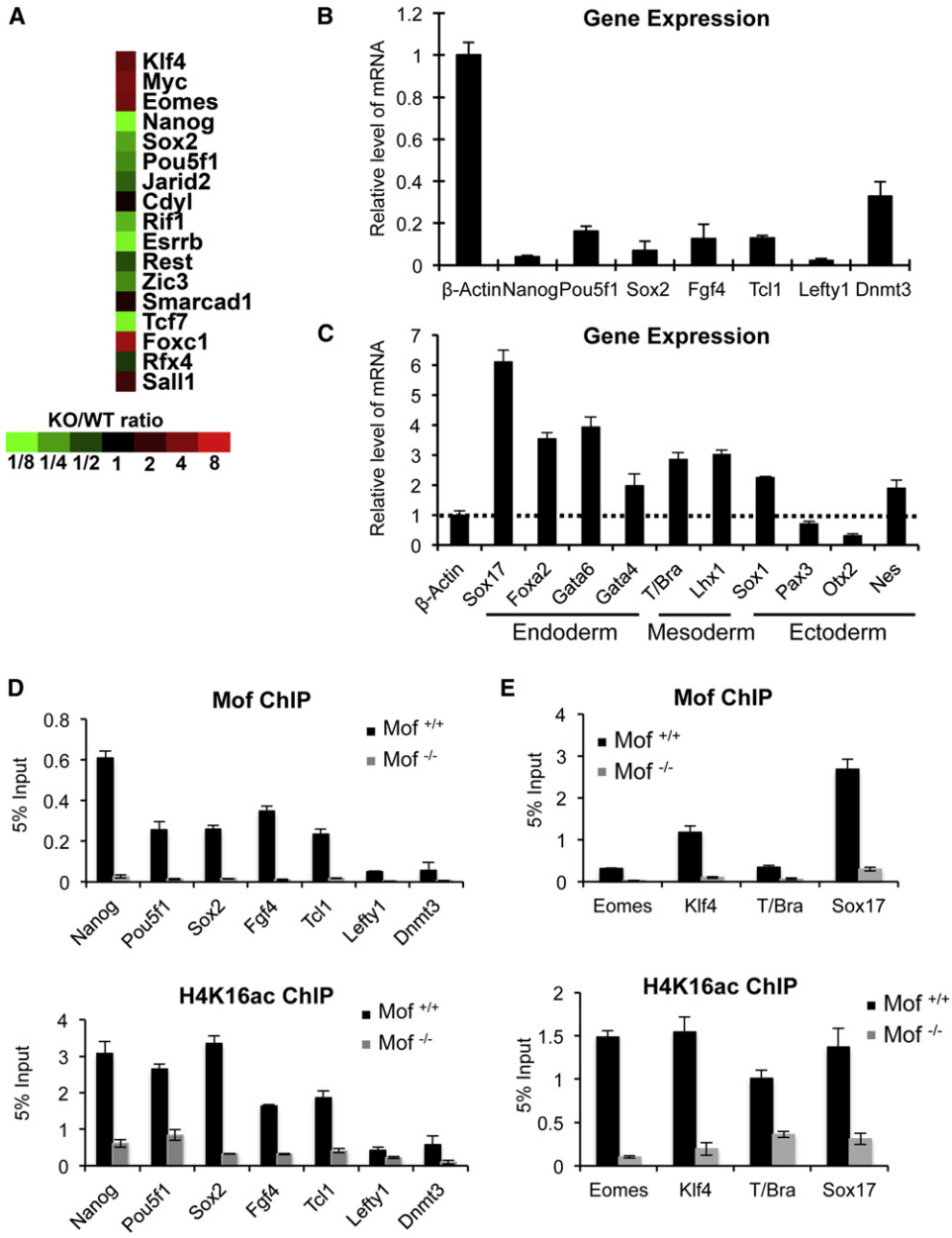

Figure 3. Mof Regulates the ESC Core Transcriptional Network

(A) Heat map of expression of conserved Nanog and Oct4 joint targets (Loh et al., 2006) in wild-type and *Mof* $^{-/-}$ ESCs. Fold change of gene expression relative to wild-type ESCs is indicated at bottom.

(B and C) Real-time PCR analyses for pluripotency (B) and differentiation genes (C) in *Mof* $^{-/-}$ and *Mof* $^{+/+}$ ESCs as indicated. All mRNA levels were normalized against β-actin and are presented as relative expression in Mof null versus wild-type ESCs.

(D) ChIP for pluripotency genes that were downregulated in *Mof* $^{-/-}$ ESCs.

(E) ChIP for differentiation genes that were upregulated in *Mof* $^{-/-}$ ESCs.

For (D and E), primer sets were designed corresponding to Mof binding peaks identified by ChIP-seq (indicated in Figure S6). The antibody is indicated at top. Signals for each experiment were normalized to 5% input. For (B)–(E), means and standard deviations (as error bars) from at least three independent experiments are presented. Also see Figure S6.

upregulated genes (i.e., Eomes, Klf4, T/Bra, and Sox17) had Mof binding at coding regions and their expression changes were concurrent with loss of Mof and H4K16ac (Figure 3E). Bindings of Mof at these genes and at Sox1, GATA4, and Nestin were also confirmed by ChIP-sequencing (ChIP-seq) analyses (Figure S6C, see below). Despite modest fold changes, these results suggest that Mof deletion can lead to both increased and decreased expression of its direct targets.

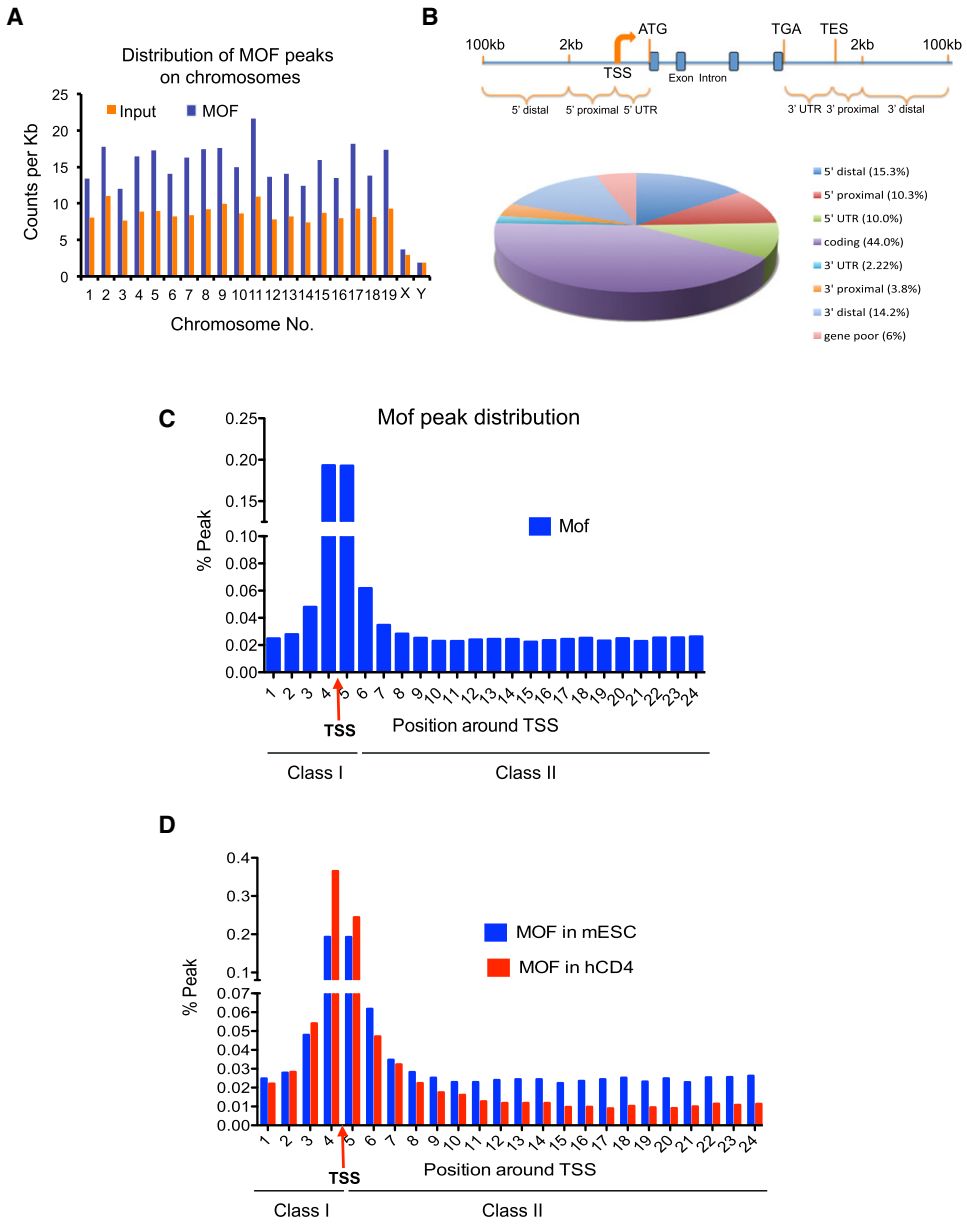

Figure 4. ChIP-Seq Analysis of Mof Binding Sites in ESCs

(A) Chromosome distribution of Mof binding peaks in mouse ESCs. y axis, count of ChIP-seq reads per kilobase. x axis, chromosome name.

(B) Distribution of Mof binding sites relative to nearest Refseq genes. Top, schematic for eight counting categories. Bottom, pie chart for percentage distribution of Mof peaks in each category.

(C) Distribution of Mof peaks in a 12 kb region from −2 kb to +10 kb around TSS (indicated by red arrow). y axis, percentage of Mof peaks relative to total Mof peaks within the defined region. x axis, bin numbers, with each representing a 500 bp region. Mof peaks are indicated as class I and class II peaks at bottom.

(D) Comparison of Mof distribution within the defined 12 kb region in mESCs (blue) and human $CD4^+$ cells (red). TSS and class I and II sites are indicated at bottom. Also see Figure S4.

Genome-wide Mapping of Mof Binding Sites in ESCs by ChIP-Seq

Increased expression of Mof direct targets in *Mof*$^{-/-}$ ESCs is surprising considering its widely accepted role as a transcription coactivator. In order to assess the function of Mof at global levels, we decided to identify Mof direct targets in murine ESC genome by ChIP-seq. ChIP-seq of input DNA was used as the control and duplicated biological samples were sequenced and analyzed. The ChIP-seq results showed that Mof distributed broadly in ESCs, enriched (over input) on all autosomes in the mammalian genome (Figure 4A). In contrast to highly enriched male X chromosome binding in *Drosophila*, Mof had minimal binding on sex chromosomes in mammal (Figure 4A). To examine Mof distribution relative to gene structure, we divided

the genome into eight categories: 5′ distal (2–100 kb upstream of transcription start site [TSS]), 5′ proximal (0–2 kb upstream of TSS), 5′ UTR (TSS to ATG), coding, 3′ UTR (TGA to transcription end site [TES]), 3′ proximal (0–2 kb downstream of TES), and 3′ distal (2–100 kb downstream of TES) regions. The rest of the loci were referred to as gene poor regions. Peak counts after normalizing against category sizes were included in Figure S4A. The majority of Mof binding sites (~56%) were mapped to the transcribed region in the genome including ~44% peaks in coding regions, ~10% in 5′ UTR and ~2% in 3′ UTR. The distribution of Mof was more pronounced toward 5′ end of genes with 20% peaks at 5′ proximal or 5′ UTR as compared to ~6% binding at 3′ UTR and 3′ proximal regions (Figure 4B). Furthermore, ~30% of Mof peaks were at either distal or gene poor regions (Figure 4B). The functional significance of gene distal binding for Mof remained to be explored. Screen shots for Mof peaks at representative genes were included in Figure S6 and Figure S7.

We further analyzed Mof binding peaks within a 12 kb region surrounding annotated TSS. To this end, Mof peaks were counted and grouped into 24 bins with 500 bp intervals starting from −2 kb to +10 kb regions. As shown in Figure 4C, Mof peaks centered on TSS and ~40% Mof peaks were within 500 bp of TSS. Furthermore, relatively low but persistent Mof binding was found throughout the 10 kb region downstream of TSS, which accumulatively accounts for 50% Mof peaks within the defined 12 kb region. To gain further insights on Mof binding in ESCs, we divided Mof peaks into two classes: class I includes peaks at −2 to +0.5 kb region (bins 1–5), representing promoter and TSS proximal Mof binding; and class II includes peaks at +0.5 to +10 kb region (bins 6–24), representing Mof binding at downstream coding region (Figure 4C and Figure S4B). We then compared our Mof ChIP-seq results with those of primary human resting $CD4^+$ cells ($hCD4^+$) (Wang et al., 2009). Consistent with ESC-specific regulation, no MOF binding was found at Nanog, Oct4, or Sox2 genes in $hCD4^+$ cells (Figure S6B, Wang et al., 2009). At global level, Mof binding in $hCD4^+$ cells was significantly enriched at the 5′ end of genes (41.8%), in contrast to 23.2% of MOF binding at coding regions (Figure S4C). The difference in Mof peak distribution between mESCs and $hCD4^+$ cells was not due to differences in category breakdown of two genomes, which was about the same (Figures S4A and S4C). Consistently, analyses of Mof peaks in the defined 12 kb region near TSS showed significant enrichment of Mof class I peaks (71.4%) and fewer class II peaks (29.6%) in the differentiated $hCD4^+$ cells as compared to mESCs (48.8% class I and 51.2% class II). The basis for different Mof distribution in these two cells remains to be decided. However, broader Mof distribution downstream of TSS is consistent with the hyper-dynamic chromatin conformation (Meshorer, 2007; Niwa, 2007) and hyperactive transcription states (Efroni et al., 2008) of ESCs.

Mof Has a Broad Role in Regulating the ESC Transcriptome

To understand the direct function of Mof in regulating the ESC transcriptome, we cross-referenced the ChIP-seq results with gene expression analyses. We found that among genes with changed expression in $Mof^{-/-}$ ESCs, 1,557 down- (~65%) and 1,295 up- (~62.5%) regulated genes had Mof binding sites (Figure 5A). Consistent with global changes in Mof transcriptome, changes in expression of Mof direct targets were modest, with mean fold change around 2.5 (Figure 7C). Gene ontology (GO) term enrichment analyses of differentially expressed Mof targets confirmed that Mof, as a general transcription cofactor, is indeed involved in many biological processes such as gene expression, cell cycle regulation, DNA repair, and the metabolic process (Table S3 and Table S4) (Li et al., 2010). These pathways were largely downregulated upon Mof deletion. When developmental pathways were examined, we found that downregulated Mof targets were highly enriched for stem cell maintenance, development, and differentiation ($p < 10^{-5}$, Figure 5B). In contrast, upregulated Mof targets were highly enriched in cellular differentiation and various developmental programs (Figure 5B). The downregulation of stem cell genes and upregulation of multilineage differentiation genes in $Mof^{-/-}$ ESCs at a global level support our results at selected gene targets. Interestingly, most of the upregulated differentiation genes shown in Figure 3 had Mof binding sites at the downstream coding regions (Figure S6).

Given the distinct Mof binding within the 12 kb region of the TSS, we further characterized Mof target genes based on whether Mof binding is in promoter and TSS proximal region (class I) or at gene bodies (class II) (Figure 5C). We found that significantly more genes with exclusive class I Mof binding sites were downregulated (824 versus 494) upon Mof deletion (single-sided Fisher's exact test, $p = 3.6e^{-6}$, Figure 5C). In contrast, a significant number of genes with exclusive class II Mof binding sites were upregulated upon Mof deletion (single-sided Fisher's exact test, $p = 0.0098$, Figure 5C). These results imply that distinct Mof binding patterns along target genes reflect a real functional difference for Mof in transcription regulation. Consistent with GO term analyses for Mof transcriptome, class II Mof targets were enriched for genes involved in cell differentiation or tissue/organ development, many of which were upregulated upon Mof deletion (data not shown).

Mof Specifically Regulates the Nanog Core Transcriptional Network

Given that Mof deletion in mESCs led to loss of self-renewal (Figure 2) and downregulation of stem cell maintenance genes (Figure 5C) including core transcription factors Nanog, Pou5f1 (Oct4), and Sox2 (Figure 3), we hypothesized that Mof may play an important role in the ESC core transcriptional network. To test this, we first compared the Mof transcriptome with those of core transcription factors reported in the literature to see if there were any interconnectivity (Ang et al., 2011; Ivanova et al., 2006; Loh et al., 2006). We performed gene set enrichment analyses (GSEA) for Mof direct targets with those of several core ESC transcription factors including Nanog, Oct4, Esrrb, Tbx3, and Sall4. Interestingly, significant enrichment was only found for Mof and Nanog transcriptome ($p < 0.00001$, Figure 5D), whereas there was no statistically significant enrichment for other ESC core transcription factors (i.e., Oct4, Esrrb, Tbx3, and Sall4) (Figure 5D and Figures S5A–S5C). Furthermore, when we performed separate GSEA for Nanog transcriptome and Mof targets that had class I or class II binding sites, only Mof targets with class I binding sites show significant enrichment of Nanog-regulated genes (Figure 5D). No enrichment between

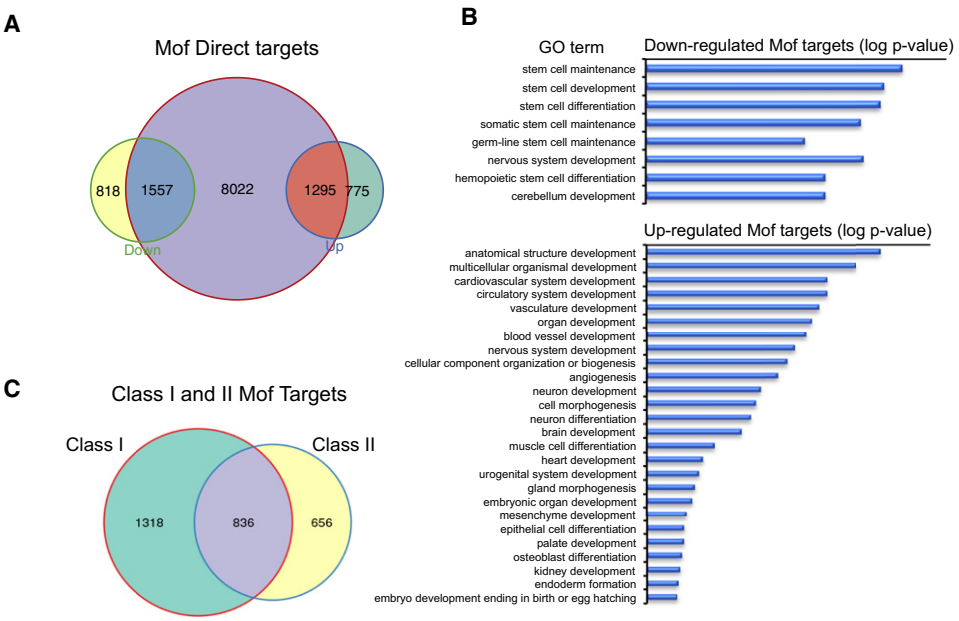

	Class I	Class I+II	Class II
Down	824	444	328
Up	494	392	328

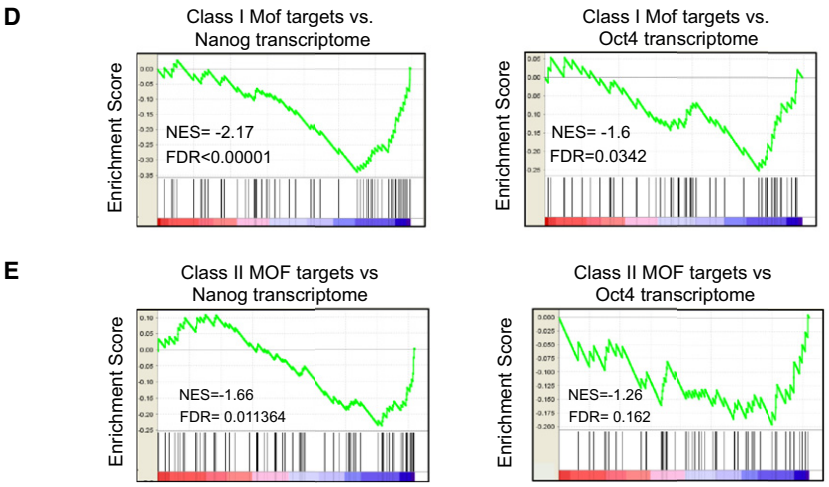

Figure 5. Mof Regulates the Nanog-Specific ESC Core Transcriptional Network

(A) Venn diagram for overlap of Mof bound genes (yellow) and genes that were either upregulated (blue) or downregulated (orange) in *Mof*$^{-/-}$ ESCs. Fisher's exact test ($p < 2.2 \times 10^{-16}$) was performed to test for statistical significance of enrichment of upregulated or downregulated genes with direct Mof binding.

(B) GO term analyses for Mof downregulated genes (top) and Mof upregulated genes (bottom). Selected developmental pathways are presented and log p value was used to rank the enrichment.

(C) Top, Venn diagram for overlap of Mof targets with class I (green) or class II (yellow) binding sites. Bottom, a table for number of genes that were upregulated or downregulated in each category.

(D and E) GSEA of Mof targets with class I binding sites (D) or class II binding sites (E) and Nanog (left) or Oct4 (right) transcriptome (Ang et al., 2011). NES, normalized enrichment score; FDR (p value), false discovery rate. Also see Figures S4 and 5.

Mof targets with class II only binding sites and Nanog transcriptome were found (p = 0.011, Figure 5E). Importantly, in corroboration with the observation that class I Mof targets were largely downregulated upon Mof deletion, correlation of Mof and Nanog transcriptome is mostly for the downregulated gene sets (NES = −2.17, Figure 5D). Similar GSEA for Oct4 transcriptome did not identify significant correlation with either class I or class II Mof targets (Figures 5D and 5E, right panel).

In addition to transcriptome analyses, we also compared Mof binding peaks with those of Nanog (Ang et al., 2011). We found

that ~79% of Nanog target genes had Mof binding (Fisher's exact test, $p < 10^{-16}$, Figure S4C). Importantly, distribution of average Mof/Nanog joint peaks showed enrichment toward 5′ end of genes compared to Mof alone peaks (Figure S4D), in agreement with our finding that genes with class I Mof binding sites are specifically involved in Nanog-dependent transcription regulation in ESCs (Figure 5D). All together, these results strongly argue that Mof is an integral part of the Nanog-mediated ESC core transcriptional network.

Overexpression of Nanog Rescues Mof Null Phenotypes in ESCs

Nanog is a highly divergent homeodomain-containing protein commonly bestowed a central position in the transcriptional network of pluripotency (Chambers et al., 2007; Mitsui et al., 2003; Silva et al., 2009). Given the direct regulation of Nanog expression by Mof (Figure 3B) and specific GSEA enrichment of Mof- and Nanog-regulated genes (Figure 5D), we decided to test whether overexpression of Nanog rescues self-renewal defects of *Mof*$^{-/-}$ ESCs. To this end, we stably transfected *Mof*$^{flox/flox}$, *Cre-ER*^{TM} cells with a Nanog-expressing vector (Ito et al., 2010). For controls, we also made cell lines that stably express wild-type Mof or Mof truncation mutant (i.e., Δ173–257aa) that is enzymatically deficient (Li et al., 2010). As shown in Figure 6A, levels of exogenous Mof, Mof mutant, and Nanog proteins were comparable to endogenous protein levels in *Mof*$^{flox/flox}$, *Cre-ER*^{TM} ESCs. Endogenous Mof was then deleted by 4-OHT treatments before the experiment. Consistent with the result that Mof regulated Nanog expression (Figure 3B), Nanog protein level was drastically lower in *Mof*$^{-/-}$ cells, which could be fully restored by expression of either wild-type Mof or exogenous Nanog. In contrast, inactive Mof mutant could not rescue Nanog expression (Figure 6A). When we examined ESC morphology, AP activity, and expression of key regulators of the rescued cell lines, we found that wild-type Mof was able to rescue most Mof null phenotypes (Figures 6B and 6C). The *Mof*$^{-/-}$ ESCs expressing exogenous Mof had indistinguishable morphology from those of wild-type ESCs (Figure 6B) and ~70%–80% of colonies were AP staining positive (Figure 6B). This result confirmed that phenotypes observed in *Mof*$^{-/-}$ ESCs were due to Mof deletion, but not other nonspecific secondary mutations. In contrast, the Mof mutant failed to rescue Mof-deficient phenotypes. The *Mof*$^{-/-}$ + *Mof*^{mut} ESCs had loose cell-cell contacts and poor AP staining, which were similar to *Mof*$^{-/-}$ ESCs (Figure 6B). This result suggests that Mof acetyltransferase activity was essential for its functions in ESCs. Strikingly, although exogenous Nanog could not rescue loss of viability associated with extended culturing of *Mof*$^{-/-}$ ESCs (data not shown), it rescued most defects associated with ESC self-renewal. About 50%–60% Nanog-expressing *Mof*$^{-/-}$ ESCs formed compact colonies and demonstrated strong AP staining, indicative of the restoration of ESC features (Figure 6B). The lower numbers of AP-positive clones from Nanog rescue cells probably result from variation in exogenous Nanog expression level and low Oct4 expression in these cells (see below). In addition to morphological changes, we also examined whether ectopic Nanog expression restored expression of Mof-dependent ESC genes. In most cases, Nanog expression led to changes in gene expression similar to that of wild-type or wild-type rescue ESCs. As shown in Figure 6C, exogenous Nanog reactivated several genes repressed in *Mof*$^{-/-}$ ESCs, including Fgf4, Lefty1, and Otx2, to the level of wild-type or wild-type Mof-rescued ESCs. The notable exception is Oct4, which remained low in Nanog-rescued *Mof*$^{-/-}$ cells (see Discussion). Similarly, Nanog suppressed induction of differentiation regulators such as Foxa2, Gata4, and Gata6 in *Mof*$^{-/-}$ ESCs (Figure 6C). One thing worth noting is that global H4K16ac remained very low in Nanog-rescued ESCs. This suggests that Mof and its acetyltransferase activity are probably required for expression of Nanog, which in turn regulates a cascade of pluripotency and/or differentiation genes. Taken together with the genomic analysis and the Nanog rescue experiment, our results suggest that Nanog is a major target and a functional mediator of Mof in ESCs.

Mof Regulates Wdr5 Binding at Key Regulatory Regions in ESCs

Several groups recently studied the function of H3K4me3 in ESCs by knocking down key components of the MLL complex Dpy30/Rbbp5 or Wdr5 (Ang et al., 2011; Jiang et al., 2011). Although knocking down these genes affected global H3K4me3, only Wdr5 knockdown significantly attenuated expression of self-renewal genes (i.e., Nanog, Oct4, and Sox2) and induction of cell differentiation (Ang et al., 2011). The differences of Wdr5 and Dpy30/Rbbp5 knockdown phenotypes in ESCs raise an interesting question: is the function of Wdr5 in ESCs solely to establish H3K4me3 or does Wdr5 play roles in other yet uncharacterized epigenetic pathways to influence ESC self-renewal? Given that Wdr5 is a stable component of the Mof-Msl1v1 complex (Dou et al., 2005; Li et al., 2009), we decided to examine whether Wdr5 plays a role in Mof-mediated ESC regulation. We first confirmed that both global H3K4me3 and Wdr5 expression were not affected by Mof deletion in ESCs (Figures S7A and S7B). We then compared Mof ChIP-seq data with that of Wdr5 and H3K4me3 in ESCs (Ang et al., 2011). We surveyed the extent that Mof binding peaks fell within 100 bp of the peak centers for Wdr5 or H3K4me3. Strikingly, Mof binding peaks physically overlapped with close to 30% of Wdr5 and 39% of H3K4me3 peaks across the genome ($p < 10^{-16}$, Pearson's Chi-square test, Figure 7A). The close proximity of these binding sites suggested that they colocalized on either the same or adjacent nucleosomes. We further analyzed the distribution of Mof/Wdr5 and Mof/H3K4me3 joint peaks along the defined 12 kb region surrounding TSS. As shown in Figure 7B, joint peaks for Mof/Wdr5 and Mof/H3K4me3 were highly enriched around TSS, with 83% (pink, 1,293 genes) and 71% (orange, 2,944 genes) peaks, respectively, in the class I region. In contrast, a larger proportion of Mof peaks without Wdr5 or H3K4me3 resides in the class II region (Figure 7B). The promoter enrichment of Mof/Wdr5 was consistent with our previous finding that the Wdr5-containing Mof-Msl1v1 complex functions in transcription initiation (Li et al., 2009).

Consistent with the observation that more genes with class I Mof peaks were downregulated, among ~491 Mof/Wdr5 joint targets that changed expression upon Mof deletion, a significant percentage of genes (306, 62.3%) were downregulated as compared to ~55% of Mof targets without Wdr5 binding

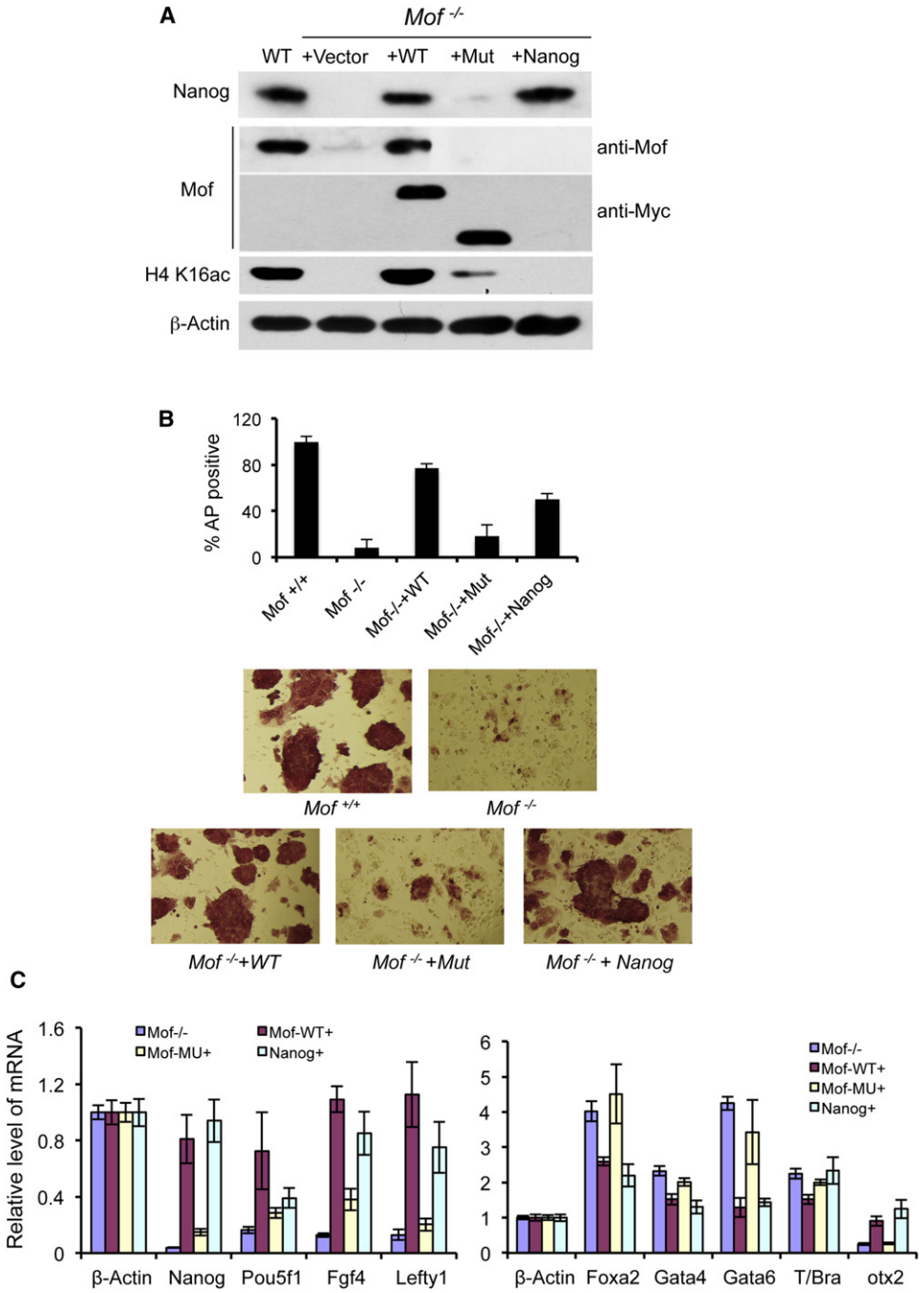

Figure 6. Nanog Overexpression Rescues Mof Null Phenotypes in ESCs

(A) Immunoblots for Nanog, Mof, and H4K16ac in wild-type or *Mof*$^{-/-}$ ESCs rescued with control vector, wild-type Mof, mutant Mof, or Nanog. Antibodies used in the experiments are indicated at right. Both exogenous wild-type and mutant Mof were Myc-tagged.

(B) AP staining of wild-type ESCs and *Mof*$^{-/-}$ ESCs expressing exogenous wild-type Mof, Mof mutant, or Nanog as indicated. Top, percentage of AP-positive clones of *Mof*$^{-/-}$ and three rescue ESCs relative to wild-type ESCs is presented. Means and standard deviations (as error bars) from two independent experiments are presented. Bottom, images (20×) for each cell lines as indicated at bottom.

(C) Real-time PCR analyses for pluripotency (left) and differentiation genes (right) in *Mof*$^{-/-}$ and three rescue cell lines as indicated. All mRNA levels were normalized against β-actin and were presented as relative fold changes to wild-type ESCs. Means and standard deviations (as error bars) from at least three independent experiments are presented. Also see Figure S3.

(single-sided Fisher's test, $p = 4.2e^{-9}$; for gene list see Table S7). Another feature of Mof/Wdr5 joint targets is that their upregulation upon Mof deletion was significantly less than Mof targets without Wdr5 binding (nonpaired Wilcoxon test, $p = 2.87e^{-6}$, Figure 7C right panel). A similar distinction of Mof/H3K4me3 joint targets was also found (nonpaired Wilcoxon test, $p = 4.58e^{-6}$,

Figure 7D right panel). Given the colocalization of Mof/Wdr5 peaks and downregulation of their targets upon Mof deletion, it is likely that regulation of the ESC core transcriptional network by Wdr5 could be partially mediated by Mof. Indeed, ChIP analyses confirmed that that binding of Wdr5 and H3K4me3 at selected pluripotent gene targets was Mof dependent. As shown in Figure 7E, Mof was essential for Wdr5 binding at the Nanog promoter (Figure 6B). Mof deletion led to both reduced Wdr5 binding and H3K4me3. Similar regulation was also observed at Sox2 and Utf1 gene promoters (Figure 7E). These results suggest that both Mof and Wdr5 are important for regulating pluripotent genes such as Nanog and Sox2 (Figure 7E). Furthermore, we also identified a couple of cases (i.e., Cbx5 and Dhx1) where Mof deletion led to reduced Wdr5 binding with no change in H3K4me3 in *Mof*$^{-/-}$ ESCs (Figure 7C), supporting the idea that Wdr5 can play roles independent of H3K4me3 at some gene promoters. All these genes had decreased expression upon Mof deletion. For controls, we performed ChIP assays for Wdr5 and H3K4me3 at several Mof targets without Wdr5 binding. At gene loci such as Mef2a, GATA4, and Klf4, Wdr5 binding was very low and did not change upon Mof deletion. However, we observed a slight increase in H3K4me3 at these loci (Figure 7E), which accompanied increased expression of these genes in *Mof*$^{-/-}$ ESCs (Table S7). Although interplays between Mof and Wdr5 binding were complex, nonetheless, we were able to establish Mof as an important upstream regulator of Wdr5 at important ESC loci.

Mof Regulates H3K4 Methylation at Some Bivalent Domains in ESCs

Since we found that H3K4me3 at some gene loci depended on Mof, we decided to further examine whether Mof is involved in setting up and/or regulating the H3K4me3 in ESCs, especially at the functionally important bivalent domains (Azuara et al., 2006; Bernstein et al., 2006). To this end, we cross-examined Mof binding peaks with reported bivalent regions (Bernstein et al., 2006). Among 8,041 peak regions that were marked with both H3K4me3 and H3K27me3, there were 2,046 peaks (~26.3%) that physically overlap with Mof binding sites (i.e., centering in the same region). A significant proportion of overlapping peaks (i.e., 564 or 27.6%) was within 2 kb of TSS ($p < 10^{-16}$; for a full list see Table S7). Among them, 106 genes were downregulated and 41 genes were upregulated in *Mof* $^{-/-}$ ESCs (Table S7), highlighting the potential regulatory role of Mof at bivalent domains in ESCs. ChIP assays for direct Mof binding and H3K4me3 and H3K27me3 at selected loci were shown in Figure S7D. Several Mof-regulated bivalent genes (e.g., Olig1 and Fgf15) have been shown to play important roles in ESC differentiation (Fischer et al., 2011; Zhou and Anderson, 2002), further supporting the importance of Mof in ESC regulation.

DISCUSSION

Nanog Is a Key Downstream Target for Mof in ESCs

Among chromatin regulators, only a handful of them have been reported to regulate ESC self-renewal (Orkin and Hochedlinger, 2011; Young, 2011). Here, we have firmly established that Mof is a critical epigenetic regulator for this important stem cell feature. ESCs with Mof deletion exhibit loss of self-renewal and aberrant expression of both pluripotency genes and differentiation marker genes. Importantly, we have shown that Mof function is largely mediated by the ESC core transcription factor Nanog. Using combined gene expression and ChIP-seq analyses for wild-type and *Mof*$^{-/-}$ ESCs, we demonstrate that Mof has a profound and direct impact on the ESC transcriptome. GSEA for Mof direct targets and the ESC core transcriptional network shows significant and specific enrichment between Mof and Nanog transcriptome (Figure 4D). The enrichment is mostly for the downregulated gene set, supporting Mof as a transcription coactivator in Nanog pathways. A prominent role of Mof in regulating the ESC transcription network is further supported by the fact that ~80% of Nanog target genes have direct Mof binding sites (Figure S5D) and ectopic expression of Nanog can partially suppress loss of the self-renewal phenotype in *Mof*$^{-/-}$ ESCs.

There are several things we would like to point out in the Nanog experiments.

First, although Mof targets overlap significantly with those of Nanog, they do not necessarily bind to the same DNA sequences. In fact, when we performed "motif" search for Mof binding sites, consensus sequences for Nanog binding sites were not identified as top hits (data not shown). It is possible that Nanog may preferably bind to genes that already have Mof bindings. The recent finding that Nanog weakly interacts with Wdr5, a Mof-interacting protein, is consistent with this scenario (Ang et al., 2011). Alternatively, given the wide distribution of Mof peaks in genome, it is possible that Mof and H4K16ac modulate the chromatin "milieu" (Orkin and Hochedlinger, 2011), which in turn influences Nanog recruitment. The exact mechanism for the functional interplays between Mof and core transcription factors in ESCs remains to be studied.

Second, Nanog expression suppressed most Mof null phenotypes without restoration of H4K16ac (Figure 6A). This result points out that although Mof is essential for regulating Nanog and/or other ESC core transcription factors, it is probably functionally redundant with other chromatin regulators in regulating downstream targets. Therefore, once Nanog protein level is restored by ectopic expression, Mof is largely dispensable for downstream regulatory events. Precedence has recently been reported for an Eed/Sox2 regulatory loop, in which overexpressing Sox2 can rescue phenotypes of Eed-deficient ESCs without restoring H3K27me3 (Ura et al., 2011). This hypothesis is further supported by previous studies that show that multiple HATs, including Tip60, p300, and Gcn5, function downstream of ONS in ESCs. These enzymes are able to acetylate histones for transcription activation. Indeed, although genetic ablation or knocking down these enzymes has no effects on expression of ONS themselves, they affect expression of ONS target genes and ESC differentiation processes to various degrees (Fazzio et al., 2008; Lin et al., 2007; Zhong and Jin, 2009). Future characterization of Nanog-dependent gene regulation in *Mof*$^{-/-}$ ESCs and interplays of Mof with other chromatin regulatory complexes at Nanog target genes will provide insights in this regard.

Third, although Nanog expression rescued most Mof null phenotypes, it failed to restore Oct4 expression in *Mof*$^{-/-}$ ESCs (Figure 6C). This result suggests that Mof regulation of Oct4 expression is independent of Nanog in ESCs. The failure

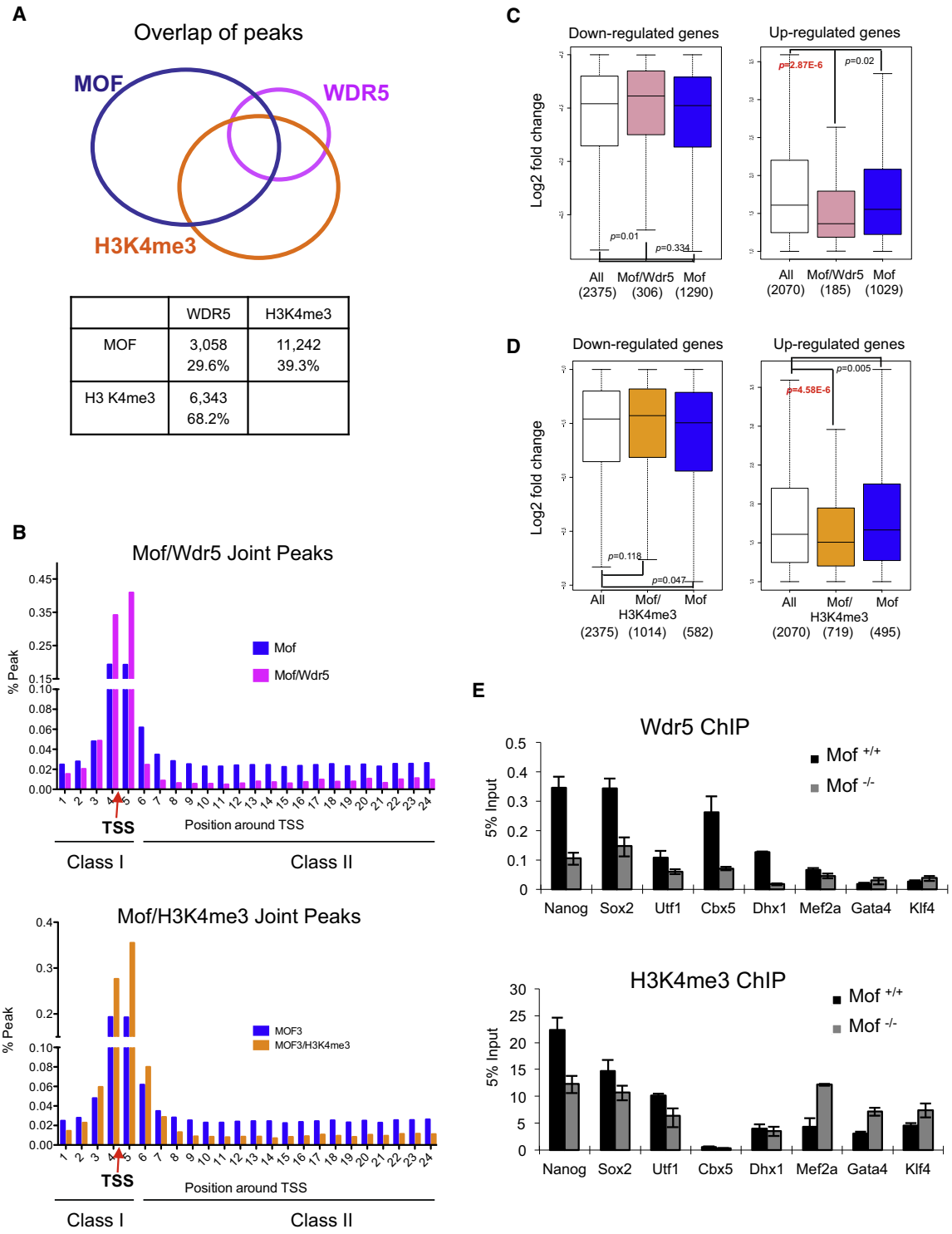

	WDR5	H3K4me3
MOF	3,058 29.6%	11,242 39.3%
H3 K4me3	6,343 68.2%	

Figure 7. Mof Regulates Wdr5 Binding at Key ESC Loci

(A) Top, Venn diagram for direct physical overlap of binding peaks for Mof (blue), Wdr5 (pink), and H3K4me3 (orange) (Ang et al., 2011). Total number and percentage of overlapping peaks relative to Wdr5, or H3K4me3 peaks, are summarized in the table below.

(B) Distribution of Mof and Mof/Wdr5 joint peaks (top) or Mof/H3K4me3 joint peaks (bottom) as class I or class II peaks. Red arrow, TSS. y axis, percentage of peaks relative to total peaks within the defined region. x axis, bins representative of a 500 bp region.

(C) The box plots for fold changes in expression of total (white), Mof/Wdr5 (pink), and Mof only (blue) target genes.

(D) The box plots for fold changes in expression of total (white), Mof/H3K4me3 (orange), and Mof only (blue) target genes. For (C) and (D), bottom and top of the boxes correspond to the 25th and 75th percentiles and the internal band is the 50th percentile (median). The plot whiskers extending outside the boxes correspond

for Nanog overexpression to restore Oct4 expression may explain partial rescue phenotypes of the *Mof*$^{-/-}$ ESCs (Figure 6B). Unexpectedly, although most Nanog-expressing *Mof* $^{-/-}$ ESCs have a low Oct4 level, they did not differentiate into the trophectoderm lineage. The levels of trophectoderm marker genes such as Hand1 and Cdx2 that were normally activated by Oct4 knockdown (Niwa et al., 2000) remained unchanged in *Mof*$^{-/-}$ ESCs (Figure S3B). This result suggests that Mof is important for activation of at least some trophectoderm markers and for differentiation of trophectoderm lineage. The requirement of Mof during cell differentiation is also supported by the fact that differentiation markers for all three germ layers are modestly but consistently downregulated by loss of a Mof allele (Figure S2). Therefore, it is likely that Mof is important for both ESC stemness and differentiation. Whether these two processes involve the same or distinct Mof complexes will be subject to future studies.

Distinctive Mof Binding in ESCs

Our ChIP-seq analyses reveal that unlike *Drosophila*, where Mof exhibits a bimodular Mof binding pattern at TSS and 3′ end of genes (Kind et al., 2008), Mof binding in mammals is enriched at TSS but also distributed evenly in downstream coding regions. The difference may be a reflection of distinct gene structures for mammal and *Drosophila*. Interestingly, we find that the elevated Mof binding at gene coding regions is a unique feature in ESCs. The coding-bound Mof accounts for ~50% of total Mof peaks within the 12 kb defined regions in ESCs whereas they comprise ~20% in hCD4^{+} cells (Figure 4D). GO term analyses for genes with coding-bound Mof show drastic differences between these two cells. When pathways specific for developmental processes are analyzed, genes with coding-bound Mof in ESCs are heavily involved in tissue/organ development and programs for multilineage cell differentiation (Figure S5A). However, those in hCD4^{+} cells are only involved in hematopoietic and lymphoid organ development and leukocyte differentiation (Figure S5A). Parallel GO term analyses on genes with TSS Mof binding show no cell-specific enrichment in differentiation (Table S5). This result shows that significant and cell-specific enrichment of Mof targets is intriguingly linked to the differentiation potential of respective cells. Since most differentiation genes are not expressed in wild-type ESCs, Mof binding serves to mark these "poised" genes for later activation.

One remaining question for this ESC-specific Mof binding pattern is how it is established and how Mof is recruited to these poised loci in ESCs. Since these loci are not actively transcribed, Mof binding at these regions cannot be simply explained as a transcription-coupled event. One feature of ESCs is their highly dynamic chromatin states. It would be interesting to test if broad binding of Mof is a result of less compact higher-order chromatin structure in ESCs and if Mof is selectively targeted to regions with yet-to-be-characterized epigenetic marks that destine genes for differentiation-induced activation. Notably, the epigenetic marks are not necessarily bivalent domains, which show no significant enrichment at Mof binding sites in ESCs.

Mof-Mediated Transcriptional Regulation in ESCs

One surprising finding of our study is that Mof deletion leads to both increased and decreased expression of its direct targets. Although we cannot rule out that gene upregulation is due to indirect effects, a significant number of upregulated genes have Mof binding sites near TSS or in gene bodies (Figure 3C). Notably, the fold changes for both the downregulation and upregulation of gene expression upon Mof deletion seem modest, with mean changes ~2.5- to 2.8-fold. It is likely that Mof functions as a chromatin modulator, regulating chromatin environment and finetuning the transcription machinery as it passes the transcribed region. The moderate effects on transcription are consistent with chromosome-wide 2-fold gene activation observed in the Mof-mediated *Drosophila* dosage compensation process. To understand whether different transcription outcome upon Mof deletion is due to regulation by distinct Mof complexes (i.e., Mof-Msl1v1 and Mof-Msl) (Li et al., 2009), we divide Mof targets based on (1) relative position of Mof binding sites to TSS and (2) whether they have Mof/Wdr5 joint peaks. The results show that genes with Mof binding exclusively at TSS are more likely to be downregulated upon Mof deletion (824 versus 494, Figure 5C). This bias is also observed for Mof/Wdr5 joint targets (306 versus 185, Figure 7C). Given that Mof/Wdr5 joint peaks are overwhelmingly located at TSS (Figure 7B), these two results corroborate with each other in supporting a specific function of the Mof-Msl1v1 complex at TSS.

On the contrary, for genes with coding-bound Mof, especially those with exclusive class II sites, Mof deletion leads to an equal chance of upregulation or downregulation (Figure 5C). These Mof targets (without Wdr5 peaks) also seem to be more upregulated upon Mof deletion compared to those with Mof/Wdr5 or Mof/H3K4me3 joint peaks (Figure 7C and data not shown). Altogether, these results argue for a distinct role for coding-bound Mof in transcription regulation. Because the Wdr5-independent Mof-Msl complex is important for transcription elongation, it is tempting to suggest that coding-bound Mof mostly resides in the Mof-Msl complex. It will be important to further dissect the Mof binding pattern and corresponding transcriptome based on the presence of other Mof-interacting proteins (i.e., MSL1–3) to prove this point in the future. Intriguingly, two recent studies on *Drosophila* DCC complex (dMof-Msl) show that components of DCC are capable of reducing gene expression in the presence of Mof and its H4K16ac activity (Prestel et al., 2010; Schiemann et al., 2010). It would be interesting to examine whether this is conserved in mammal and whether MSL proteins serve to restrain expression of some Mof-Msl targets in ESCs. In the latter case, Mof deletion could lead to the disassembly of the Mof-Msl complex and thus relieve the repressive effects of MSL proteins at specific loci.

to the lowest and highest datum within 1.5 interquartile ranges. p values were calculated using nonpaired Wilcoxon tests as indicated. The number of genes in each category is indicated at bottom. Left, downregulated gene set. Right, upregulated gene set.
(E) ChIP experiments for Wdr5 (top) and H3K4me3 (bottom) at selected joint target genes in wild-type and *Mof* $^{-/-}$ ESCs. The antibodies used for ChIP are indicated at top. Signals for each experiment were normalized to 5% input. Means and standard deviations (as error bars) from at least three independent experiments are presented. Also see Figure S7.

Mof, H3K4me3, and ESC Regulation

Several recent studies explored the function of another transcription-activation-related chromatin modification, H3K4me3, in ESC regulation. One group showed that knocking down Wdr5, a component of the MLL methyltransferase, significantly attenuated expression of self-renewal genes (i.e., Nanog, Oct4, and Sox2) and resulted in loss of pluripotency and induction of cell differentiation (Ang et al., 2011). However, another group showed that knocking down Dpy30 and Rbbp5 in the same complexes had minimal effects on ESC self-renewal and ONS expression despite reduction of both global and loci-specific H3K4me3 (Jiang et al., 2011). The differences of Wdr5 and Dpy30/Rbbp5 knockdown phenotypes in ESCs raise an interesting question: does the H3K4me3-independent function of Wdr5 contribute to ESC regulation? In light of our results here, one likely explanation for the reported paradoxical observation is that Wdr5 functions as part of the Mof complex to regulate transcription in ESCs. This explains why Wdr5 depletion has broader ESC phenotypes than knocking down Dpy30 or RbbP5. In support, we show that Mof deletion affects Wdr5 recruitment at important gene loci, including Nanog and Sox2, and at some loci, changes in Wdr5 binding and gene expression (e.g., Cbx5) are not always accompanied by changes in H3K4me3 (Figure 7C). Future studies on the detailed mechanisms of how Mof and H3K4me3 coordinate to activate ONS genes and how Wdr5 contributes to Mof function in this context will provide insights in this aspect. The ability of Mof to regulate Wdr5 and H3K4me3 at some loci in ESCs has prompted us to examine its role at setting up the bivalent domains, epigenetic regulatory elements that govern ESC transcription program (Azuara et al., 2006; Bernstein et al., 2006). Indeed, we find that Mof regulates H3K4me3 at some important bivalent domains including those at the promoters of Nanog and Sox2 (Figure 7D). Genome-wide analyses further support extensive interconnection between Mof and H3K4me3 in ESCs (Figure 7A). Importantly, deletion of Mof in ESCs leads to aberrant expression for genes with nearby bivalent domains (Figure 7D and Table S7). The close interactions between Mof and Wdr5/H3K4me3 probably underlie the essential functions of Mof in regulating ONS expression and their regulatory circuitry.

EXPERIMENTAL PROCEDURES

Generation of ESC Lines and ESC Differentiation

Inducible Cre-expressing mouse line *CAGG Cre-ER^{TM}* was as previously described (Li et al., 2010). The *Mof* ESC lines were derived from the inner cell mass of 3.5 dpc blastocysts, which were obtained from timed mating of *Mof$^{flox/flox}$*; *CAGG Cre-ER^{TM}* mice.

AP Staining of ESCs

The Stemgent™ Alkaline Phosphatase (AP) Staining Kit was used for the detection of the AP activity according to the manufacturer's instructions. For AP staining, 1,000 ESCs for each genotype were plated and cultured with or without 4-OHT for 4 days before the staining.

Immunoblot, Quantitative RT-PCR, and ChIP Analyses

These experiments were performed as previously described (Byun et al., 2009; Dou et al., 2006). Anti-Mof (Santa Cruz), anti-H4K16ac (Millipore), anti-H3K27me3 (Millipore), anti-H3K4me3 (Millipore), anti-Wdr5 (Millipore), and anti-mouse or anti-rabbit IgG (Sigma) antibodies were used. All RT and ChIP-PCR primers are listed in the Supplemental Experimental Procedures.

Gene Expression Microarray, GO, and GSEA Analyses

Microarray analyses for wild-type and Mof null ESCs (GSE37268) were performed on Affymetrix GeneChip Mouse Genome 430 2.0 arrays (Affymetrix). The expression change of a gene was calculated using the geometric mean of all probes aligned on the gene. R package GOstats (Falcon and Gentleman, 2007) and GO.db (http://stuff.mit.edu/afs/athena.mit.edu/software/) were used for GO term association studies. For each gene list, conditional single-sided hypergeometric tests were used to calculate the p value of GO term enrichment. GSEA (Isakoff et al., 2005) was performed using JavaGSEA software provided by http://www.broadinstitute.org/gsea/. GSEA was of two gene sets representing differentially expressed genes ranked as a list by fold changes. GSEA was run on this preranked list with the number of permutations equaling 1,000.

ChIP-Seq Analyses

ChIP-seq analysis for Mof (GSE37268) was performed at NCI Sequencing Facility. Images acquired were processed through the image extraction pipeline and aligned to mouse NCBI build mm9 using ELAND. Peaks were called using HPeak (Qin et al., 2010), a hidden Markov model-based software program for identifying ChIP-enriched regions. Pearson's Chi-square test with Yates' continuity correction or Fisher exact test was used for calculating p values when evaluating overlaps between lists of genes.

ACCESSION NUMBERS

The data gathered over the course of this experiment have been deposited in NCBI's Gene Expression Omnibus and are accessible through GEO Series accession number GSE37268.

SUPPLEMENTAL INFORMATION

Supplemental Information for this article includes seven figures, Supplemental Experimental Procedures, and seven tables and can be found with this article online at http://dx.doi.org/10.1016/j.stem.2012.04.023.

ACKNOWLEDGMENTS

We thank Dr. Yi Zhang for the anti-Nanog antibody and the Nanog expression vector. This work is supported by NIGMS (R01GM082856) and American Cancer Society (RSG 117573) grants to Y.D., NHGRI (R01HG005119) grant to Z.Q., and NSFC (31171428) grant to X.L.

Received: August 28, 2011
Revised: January 7, 2012
Accepted: April 18, 2012
Published: August 2, 2012

REFERENCES

Ang, Y.S., Tsai, S.Y., Lee, D.F., Monk, J., Su, J., Ratnakumar, K., Ding, J., Ge, Y., Darr, H., Chang, B., et al. (2011). Wdr5 mediates self-renewal and reprogramming via the embryonic stem cell core transcriptional network. Cell *145*, 183–197.

Aoto, T., Saitoh, N., Ichimura, T., Niwa, H., and Nakao, M. (2006). Nuclear and chromatin reorganization in the MHC-Oct3/4 locus at developmental phases of embryonic stem cell differentiation. Dev. Biol. *298*, 354–367.

Azuara, V., Perry, P., Sauer, S., Spivakov, M., Jørgensen, H.F., John, R.M., Gouti, M., Casanova, M., Warnes, G., Merkenschlager, M., and Fisher, A.G. (2006). Chromatin signatures of pluripotent cell lines. Nat. Cell Biol. *8*, 532–538.

Bernstein, B.E., Mikkelsen, T.S., Xie, X., Kamal, M., Huebert, D.J., Cuff, J., Fry, B., Meissner, A., Wernig, M., Plath, K., et al. (2006). A bivalent chromatin structure marks key developmental genes in embryonic stem cells. Cell *125*, 315–326.

Byun, J.S., Wong, M.M., Cui, W., Idelman, G., Li, Q., De Siervi, A., Bilke, S., Haggerty, C.M., Player, A., Wang, Y.H., et al. (2009). Dynamic bookmarking

of primary response genes by p300 and RNA polymerase II complexes. Proc. Natl. Acad. Sci. USA *106*, 19286–19291.

Chambers, I., Silva, J., Colby, D., Nichols, J., Nijmeijer, B., Robertson, M., Vrana, J., Jones, K., Grotewold, L., and Smith, A. (2007). Nanog safeguards pluripotency and mediates germline development. Nature *450*, 1230–1234.

Chen, X., Xu, H., Yuan, P., Fang, F., Huss, M., Vega, V.B., Wong, E., Orlov, Y.L., Zhang, W., Jiang, J., et al. (2008). Integration of external signaling pathways with the core transcriptional network in embryonic stem cells. Cell *133*, 1106–1117.

Conrad, T., and Akhtar, A. (2011). Dosage compensation in Drosophila melanogaster: epigenetic fine-tuning of chromosome-wide transcription. Nat. Rev. Genet. *13*, 123–134.

Dou, Y., Milne, T.A., Tackett, A.J., Smith, E.R., Fukuda, A., Wysocka, J., Allis, C.D., Chait, B.T., Hess, J.L., and Roeder, R.G. (2005). Physical association and coordinate function of the H3 K4 methyltransferase MLL1 and the H4 K16 acetyltransferase MOF. Cell *121*, 873–885.

Dou, Y., Milne, T.A., Ruthenburg, A.J., Lee, S., Lee, J.W., Verdine, G.L., Allis, C.D., and Roeder, R.G. (2006). Regulation of MLL1 H3K4 methyltransferase activity by its core components. Nat. Struct. Mol. Biol. *13*, 713–719.

Efroni, S., Duttagupta, R., Cheng, J., Dehghani, H., Hoeppner, D.J., Dash, C., Bazett-Jones, D.P., Le Grice, S., McKay, R.D., Buetow, K.H., et al. (2008). Global transcription in pluripotent embryonic stem cells. Cell Stem Cell *2*, 437–447.

Falcon, S., and Gentleman, R. (2007). Using GOstats to test gene lists for GO term association. Bioinformatics *23*, 257–258.

Fazzio, T.G., Huff, J.T., and Panning, B. (2008). An RNAi screen of chromatin proteins identifies Tip60-p400 as a regulator of embryonic stem cell identity. Cell *134*, 162–174.

Feng, B., Ng, J.H., Heng, J.C., and Ng, H.H. (2009). Molecules that promote or enhance reprogramming of somatic cells to induced pluripotent stem cells. Cell Stem Cell *4*, 301–312.

Fischer, T., Faus-Kessler, T., Welzl, G., Simeone, A., Wurst, W., and Prakash, N. (2011). Fgf15-mediated control of neurogenic and proneural gene expression regulates dorsal midbrain neurogenesis. Dev. Biol. *350*, 496–510.

Gaspar-Maia, A., Alajem, A., Meshorer, E., and Ramalho-Santos, M. (2011). Open chromatin in pluripotency and reprogramming. Nat. Rev. Mol. Cell Biol. *12*, 36–47.

Gelbart, M.E., and Kuroda, M.I. (2009). Drosophila dosage compensation: a complex voyage to the X chromosome. Development *136*, 1399–1410.

Gupta, A., Guerin-Peyrou, T.G., Sharma, G.G., Park, C., Agarwal, M., Ganju, R.K., Pandita, S., Choi, K., Sukumar, S., Pandita, R.K., et al. (2008). The mammalian ortholog of Drosophila MOF that acetylates histone H4 lysine 16 is essential for embryogenesis and oncogenesis. Mol. Cell. Biol. *28*, 397–409.

Isakoff, M.S., Sansam, C.G., Tamayo, P., Subramanian, A., Evans, J.A., Fillmore, C.M., Wang, X., Biegel, J.A., Pomeroy, S.L., Mesirov, J.P., and Roberts, C.W. (2005). Inactivation of the Snf5 tumor suppressor stimulates cell cycle progression and cooperates with p53 loss in oncogenic transformation. Proc. Natl. Acad. Sci. USA *102*, 17745–17750.

Ito, S., D'Alessio, A.C., Taranova, O.V., Hong, K., Sowers, L.C., and Zhang, Y. (2010). Role of Tet proteins in 5mC to 5hmC conversion, ES-cell self-renewal and inner cell mass specification. Nature *466*, 1129–1133.

Ivanova, N., Dobrin, R., Lu, R., Kotenko, I., Levorse, J., DeCoste, C., Schafer, X., Lun, Y., and Lemischka, I.R. (2006). Dissecting self-renewal in stem cells with RNA interference. Nature *442*, 533–538.

Jiang, H., Shukla, A., Wang, X., Chen, W.Y., Bernstein, B.E., and Roeder, R.G. (2011). Role for Dpy-30 in ES cell-fate specification by regulation of H3K4 methylation within bivalent domains. Cell *144*, 513–525.

Kind, J., Vaquerizas, J.M., Gebhardt, P., Gentzel, M., Luscombe, N.M., Bertone, P., and Akhtar, A. (2008). Genome-wide analysis reveals MOF as a key regulator of dosage compensation and gene expression in Drosophila. Cell *133*, 813–828.

Kobayakawa, S., Miike, K., Nakao, M., and Abe, K. (2007). Dynamic changes in the epigenomic state and nuclear organization of differentiating mouse embryonic stem cells. Genes Cells *12*, 447–460.

Li, X., and Dou, Y. (2010). New perspectives for the regulation of acetyltransferase MOF. Epigenetics *5*, 5.

Li, X., Wu, L., Corsa, C.A., Kunkel, S., and Dou, Y. (2009). Two mammalian MOF complexes regulate transcription activation by distinct mechanisms. Mol. Cell *36*, 290–301.

Li, X., Corsa, C.A., Pan, P.W., Wu, L., Ferguson, D., Yu, X., Min, J., and Dou, Y. (2010). MOF and H4 K16 acetylation play important roles in DNA damage repair by modulating recruitment of DNA damage repair protein Mdc1. Mol. Cell. Biol. *30*, 5335–5347.

Lin, W., Srajer, G., Evrard, Y.A., Phan, H.M., Furuta, Y., and Dent, S.Y. (2007). Developmental potential of Gcn5(-/-) embryonic stem cells in vivo and in vitro. Dev. Dyn. *236*, 1547–1557.

Loh, Y.H., Wu, Q., Chew, J.L., Vega, V.B., Zhang, W., Chen, X., Bourque, G., George, J., Leong, B., Liu, J., et al. (2006). The Oct4 and Nanog transcription network regulates pluripotency in mouse embryonic stem cells. Nat. Genet. *38*, 431–440.

Lucchesi, J.C., Kelly, W.G., and Panning, B. (2005). Chromatin remodeling in dosage compensation. Annu. Rev. Genet. *39*, 615–651.

Macarthur, B.D., Ma'ayan, A., and Lemischka, I.R. (2009). Systems biology of stem cell fate and cellular reprogramming. Nat. Rev. Mol. Cell Biol. *10*, 672–681.

Meshorer, E. (2007). Chromatin in embryonic stem cell neuronal differentiation. Histol. Histopathol. *22*, 311–319.

Mitsui, K., Tokuzawa, Y., Itoh, H., Segawa, K., Murakami, M., Takahashi, K., Maruyama, M., Maeda, M., and Yamanaka, S. (2003). The homeoprotein Nanog is required for maintenance of pluripotency in mouse epiblast and ES cells. Cell *113*, 631–642.

Niwa, H. (2007). Open conformation chromatin and pluripotency. Genes Dev. *21*, 2671–2676.

Niwa, H., Miyazaki, J., and Smith, A.G. (2000). Quantitative expression of Oct-3/4 defines differentiation, dedifferentiation or self-renewal of ES cells. Nat. Genet. *24*, 372–376.

Orkin, S.H., and Hochedlinger, K. (2011). Chromatin connections to pluripotency and cellular reprogramming. Cell *145*, 835–850.

Orkin, S.H., Wang, J., Kim, J., Chu, J., Rao, S., Theunissen, T.W., Shen, X., and Levasseur, D.N. (2008). The transcriptional network controlling pluripotency in ES cells. Cold Spring Harb. Symp. Quant. Biol. *73*, 195–202.

Pan, G., Tian, S., Nie, J., Yang, C., Ruotti, V., Wei, H., Jonsdottir, G.A., Stewart, R., and Thomson, J.A. (2007). Whole-genome analysis of histone H3 lysine 4 and lysine 27 methylation in human embryonic stem cells. Cell Stem Cell *1*, 299–312.

Park, S.H., Park, S.H., Kook, M.C., Kim, E.Y., Park, S., and Lim, J.H. (2004). Ultrastructure of human embryonic stem cells and spontaneous and retinoic acid-induced differentiating cells. Ultrastruct. Pathol. *28*, 229–238.

Prestel, M., Feller, C., Straub, T., Mitlöhner, H., and Becker, P.B. (2010). The activation potential of MOF is constrained for dosage compensation. Mol. Cell *38*, 815–826.

Qin, Z.S., Yu, J., Shen, J., Maher, C.A., Hu, M., Kalyana-Sundaram, S., Yu, J., and Chinnaiyan, A.M. (2010). HPeak: an HMM-based algorithm for defining read-enriched regions in ChIP-Seq data. BMC Bioinformatics *11*, 369.

Robinson, P.J., An, W., Routh, A., Martino, F., Chapman, L., Roeder, R.G., and Rhodes, D. (2008). 30 nm chromatin fibre decompaction requires both H4-K16 acetylation and linker histone eviction. J. Mol. Biol. *381*, 816–825.

Ruthenburg, A.J., Li, H., Milne, T.A., Dewell, S., McGinty, R.K., Yuen, M., Ueberheide, B., Dou, Y., Muir, T.W., Patel, D.J., and Allis, C.D. (2011). Recognition of a mononucleosomal histone modification pattern by BPTF via multivalent interactions. Cell *145*, 692–706.

Schiemann, A.H., Li, F., Weake, V.M., Belikoff, E.J., Klemmer, K.C., Moore, S.A., and Scott, M.J. (2010). Sex-biased transcription enhancement by a 5′ tethered Gal4-MOF histone acetyltransferase fusion protein in Drosophila. BMC Mol. Biol. *11*, 80.

Shogren-Knaak, M., Ishii, H., Sun, J.M., Pazin, M.J., Davie, J.R., and Peterson, C.L. (2006). Histone H4-K16 acetylation controls chromatin structure and protein interactions. Science *311*, 844–847.

Silva, J., Nichols, J., Theunissen, T.W., Guo, G., van Oosten, A.L., Barrandon, O., Wray, J., Yamanaka, S., Chambers, I., and Smith, A. (2009). Nanog is the gateway to the pluripotent ground state. Cell *138*, 722–737.

Thomas, T., Dixon, M.P., Kueh, A.J., and Voss, A.K. (2008). Mof (MYST1 or KAT8) is essential for progression of embryonic development past the blastocyst stage and required for normal chromatin architecture. Mol. Cell. Biol. *28*, 5093–5105.

Ura, H., Murakami, K., Akagi, T., Kinoshita, K., Yamaguchi, S., Masui, S., Niwa, H., Koide, H., and Yokota, T. (2011). Eed/Sox2 regulatory loop controls ES cell self-renewal through histone methylation and acetylation. EMBO J. *30*, 2190–2204.

Wang, Z., Zang, C., Cui, K., Schones, D.E., Barski, A., Peng, W., and Zhao, K. (2009). Genome-wide mapping of HATs and HDACs reveals distinct functions in active and inactive genes. Cell *138*, 1019–1031.

Wu, L., Zee, B.M., Wang, Y., Garcia, B.A., and Dou, Y. (2011). The RING finger protein MSL2 in the MOF complex is an E3 ubiquitin ligase for H2B K34 and is involved in crosstalk with H3 K4 and K79 methylation. Mol. Cell *43*, 132–144.

Young, R.A. (2011). Control of the embryonic stem cell state. Cell *144*, 940–954.

Zhong, X., and Jin, Y. (2009). Critical roles of coactivator p300 in mouse embryonic stem cell differentiation and Nanog expression. J. Biol. Chem. *284*, 9168–9175.

Zhou, Q., and Anderson, D.J. (2002). The bHLH transcription factors OLIG2 and OLIG1 couple neuronal and glial subtype specification. Cell *109*, 61–73.